RSC Advances

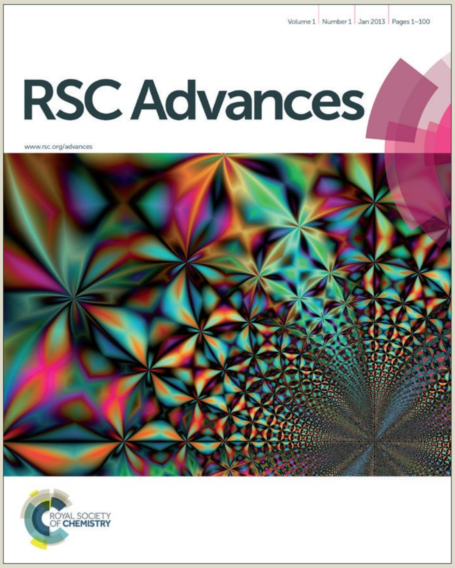

ROYAL SOCIETY OF CHEMISTRY

www.rsc.org/advances

RSC Advance

ARTICLE

Compositional dependence of electrocaloric effect in lead-free (1-x)Ba($Zr_{0.2}Ti_{0.8}$)O_3 -x($Ba_{0.7}Ca_{0.3}$)TiO_3 ceramics

Received 00th January 20xx,
Accepted 00th January 20xx

DOI: 10.1039/x0xx00000x

www.rsc.org/

Yingze Zhou,[a] Qianru Lin,[a] Wenfeng Liu[b] and Danyang Wang[*a]

We studied the electrocaloric effect (ECE) in (1-x)Ba($Zr_{0.2}Ti_{0.8}$)O_3-x($Ba_{0.7}Ca_{0.3}$)TiO_3 (BZT-xBCT) ceramics over a wide composition range (x = 0.3 - 0.7) using an indirect method based on the thermodynamics Maxwell relations. The maximum adiabatic temperature change ΔT was found to shift from the proximity of Curie temperature to higher temperatures, owing to a synergistic effect of field induced change in the phase transition temperature and alignment and growth of polar nano-regions. Coexistence of positive and negative ECEs were confirmed in BCT-rich compositions (x ≥ 0.5). The abnormal negative ECE is presumably attributed to the rhombohedral to tetragonal transition occurred at relatively low temperatures. The most promising ECE was found in BZT-0.4BCT ceramics, which exhibited a uniform ECE in the temperature range of interest, with a promising ΔT of 0.58 K at ~ 125 °C under a moderate electric field of 28 kV/cm.

Introduction

Because of the increasing environmental and ecological concerns over the conventional refrigeration systems, electrocaloric effect (ECE) has been intensively studied as an alternative cooling technology over the past decade.[1-3] ECE is an adiabatic temperature change (ΔT) or an isothermal entropy change (ΔS) of a polar material due to the change of polarization under an applied electric field.[4-6] The ECE is largest in the polar dielectric undergoing order-disorder phase transition (i.e. first-order phase transition),[4] owing to the electric field induced large entropy change associated with polarization change. Therefore, it is advantageous to employ ferroelectric materials and operate them at temperatures slightly above the ferroelectric-paraelectric transition, where the dipole alignment translates from the ordered state to disordered state, resulting in a large entropy and adiabatic temperature change.

Very recently, relaxor ferroelectrics were regarded as promising candidates for high performance ECE materials due to the fact that many relaxor ferroelectrics exhibit superior pyroelectric properties, which is the physical inverse of ECE.[7,8] Relaxor is a special class of disordered materials in which local inhomogeneities known as polar nano-regions (PNR) are formed. The local structure of PNR is usually different from the average lattice structure of the matrix in which they reside. In this sense, relaxors offer additional degrees of freedom due to their nanoscopic structures which can be converted into a ferroelectric state through applying an electric field. Large entropy changes during this process will substantially enhance the ECE.[7,9,10]

Up to now, many studies on ECE in relaxors have focused on lead-containing compounds such as $PbMg_{1/3}Nb_{2/3}O_3$-$PbTiO_3$ (PMN-PT)[9,11,12], (Pb,La)(Zr,Ti)O_3 (PLZT)[13] and polymeric materials such as P(VDF-TrFE)[3]. Although encouraging results have been obtained, the restriction of aforementioned materials lies in either the toxicity of lead or the low electrocaloric coefficient in polymer-based materials, i.e. very high electric field is required to excite the large adiabatic temperature change. Over the past decade, many efforts were made to identify lead-free replacements. Among the many lead-free relaxor systems, a large ECE is expected in those compositions, where polar and non-polar regions coexist in a broad temperature range and a first order field-induced transition from a highly disordered to the ordered state occurs at relatively low electric fields.

(1-x)Ba($Zr_{0.2}Ti_{0.8}$)O_3-x($Ba_{0.7}Ca_{0.3}$)TiO_3 [henceforth BZT-xBCT] ceramic system is a very promising lead-free piezoelectric candidate.[14] Soft dielectric relaxation behaviour is also expected in BZT-xBCT system due to hopping of the off-centred Ti^{4+} ions.[15] BZT-xBCT shows a complex phase diagram with a morphotropic phase boundary (MPB) between compositions of rhombohedral and tetragonal phases. Compounds near the MPB (x = 0.5) exhibit large dielectric permittivity in a broad temperature interval and giant electromechanical strain, which is related to a field induced transition from a non-polar into a ferroelectric state. Such transformation is expected to accompany with a large jump of entropy, which is a prerequisite for a large ECE.

---

[a] School of Materials Science and Engineering, The University of New South Wales, Sydney, NSW 2052, Australia
[b] State Key Laboratory of Electrical Insulation and Power Equipment, Xi'an Jiaotong University, Xi'an 710049, China
[*] Corresponding authors: E-mail: dy.wang@unsw.edu.au

A number of studies on the ECE in BZT-xBCT have been reported, [15-18] but the great scarcity of available data restricts our understanding on their behaviour and technological potential. In order to achieve an optimal electrocaloric performance and gain a deeper understanding on the underlying mechanisms of improving ECE, it is critical to establish a composition-structure-ECE relationship in BZT-xBCT system. In this work, electrocaloric properties of BZT-xBCT ceramics with a wide composition range were studied by indirect method. Although very high EC responses have been indirectly measured in various normal and relaxor ferroelectric thin films, [19-21] their “giant” ECEs can be mostly explained by the high dielectric breakdown strength of thin films, i.e. high ΔT can be simply achieved by large electric fields. In this work, we will focus on BZT-xBCT bulk ceramics, since only bulk materials with strong ECE would exhibit enough cooling capacity for applications in the large-scale refrigeration industry. [5]

Experimental

The BZT-xBCT (x = 0.3, 0.4, 0.5, 0.6 and 0.7) ceramics were prepared by a conventional solid state reaction route. Details of the BZT-xBCT ceramic processing can be found elsewhere. [14] The investigated compositions were located in the vicinity of the MPB, giving insight into the impact of crystal structure on the electrocaloric behaviour. The phase structure of the BZT-xBCT samples was analysed using X-ray diffractometer (PANalytical Xpert MPD). Density of the samples was measured using Archimedes method and the result was found to be between 5.32 and 5.42 g/cm^3 (~ 95% of the theoretical density) for all the samples. The specific heat capacity was measured by Simultaneous Thermal Analyzer (STA/TG-MS 449 F1 Jupiter, NETZSCH). The temperature dependence of dielectric permittivity measurements were performed using a precision impedance analyser (Agilent 4294A) connected with a temperature-controlled chamber over a temperature range of -200 ℃ to 150 ℃. The polarization versus electric field (*P-E*) hysteresis loops were measured at 1 Hz using TF Analyzer 2000 (aixACCT GmbH, Germany) from 25 ℃ up to 150 ℃ with an interval of 5 ℃.

Results and discussion

Fig.1 (a) shows the XRD θ-2θ scan patterns for BZT-xBCT ceramics measured at room temperature (25 ℃). All samples exhibit well defined perovskite structure without any impurity or secondary phase in the detection limit. It is observed that the XRD peaks shifted to higher 2θ angles with increasing BCT content, which could be attributed to the substitutions of the relatively smaller Ca^{2+} and Ti^{4+} ions, replacing Ba^{2+} and Zr^{4+} ions on the A site and B site, respectively, of the perovskite structure. Fig.1 (b) shows the evolution of pseudo-cubic $(200)_c$ peak of BZT-xBCT with the change of composition. Typical rhombohedral (R) phase is identified in BZT-0.3BCT and BZT-0.4BCT. The considerable splitting of the $(200)_c$ peaks at x = 0.6 and 0.7 suggests a tetragonal (T) symmetry. Distortion of the $(200)_c$ peak of BZT-0.5BCT implies a transformation from single R phase to a mixture of R and T phases, which is the signature of MPB.[14]

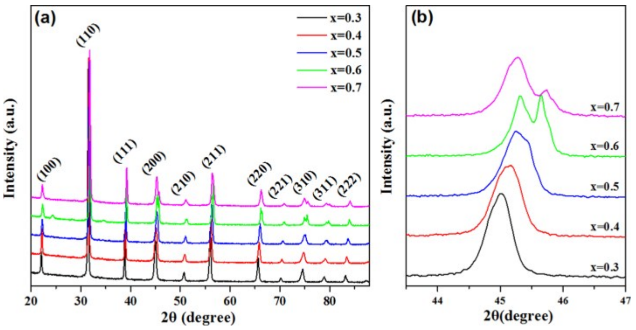

Fig. 1 (a) XRD θ-2θ scan patterns for BZT-xBCT ceramics. (b) Evolution of pseudo-cubic $(200)_c$ peaks as function of composition x.

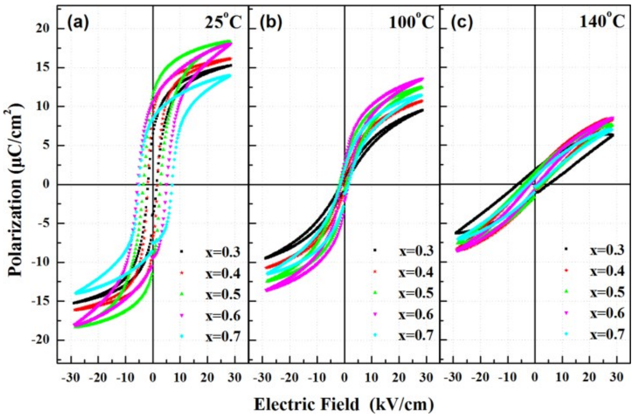

Fig.2 Ferroelectric *P-E* loops of BZT-xBCT ceramics under 28 kV/cm at (a) 25 ℃, (b) 100 ℃ and (c) 140 ℃.

The ferroelectric *P-E* hysteresis loops were measured at different temperatures in order to evaluate the ECE. Fig.2 shows the typical *P-E* loops of BZT-xBCT ceramics under a moderate electric field of 28 kV/cm measured at 25 ℃, 100 ℃ and 140 ℃ , respectively. All the compositions were characterized with electric fields up to 28 kV/cm because higher electric fields may induce significant Joule heating at high temperatures. The BZT-xBCT ceramics exhibit well-defined *P-E* loops as shown in Fig.2 (a), confirming the good ferroelectricity for all the compositions at room temperature. The *P-E* loops become slimmer as temperature increases, indicating a transition from ferroelectric to paraelectric phase. It should be noted, however, weak ferroelectricity is maintained in all the samples even when the temperature is well above their phase transition temperatures as shown in Fig.2 (c), implying a relaxor behaviour in BZT-xBCT ceramics.[22]

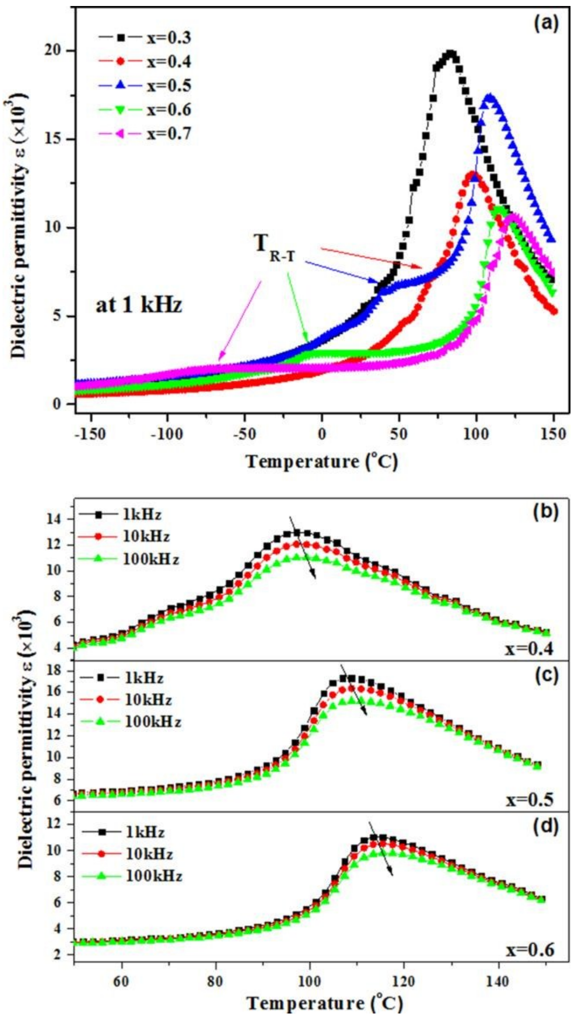

Fig.3 (a) Temperature dependence of dielectric permittivity (ε) of BZT-xBCT ceramics at 1 kHz; Dielectric permittivity as a function of temperature (50 - 150 ℃) at different frequencies (1 kHz, 10 kHz and 100 kHz) for (b) x = 0.4, (c) x = 0.5 and (d) x = 0.6. The arrow indicates the direction of increasing frequency.

Fig.3 (a) shows the temperature dependence of dielectric permittivity ($\boldsymbol{\varepsilon}$) for BZT-xBCT at frequency of 1 kHz. Obvious dielectric maxima can be found on $\boldsymbol{\varepsilon}$ - T curves for each composition (denoted by dielectric constant maximum temperature T_m) corresponding to ferroelectric-paraelectric phase transition temperature. A less conspicuous dielectric anomaly, indicating the phase transition from the rhombohedral ferroelectric phase to the tetragonal ferroelectric phase, is also observed in compositions x ≥ 0.4. The difference between these two phase transition temperatures increases with increasing BCT content x, which may possibly affects the ECE of the BZT-xBCT ceramics. Broad and slightly frequency dispersive permittivity peaks, which is one of the defining features of relaxors, can be seen at temperatures around T_m in the samples with compositions in the vicinity of MPB, as shown in Fig.3 (b) - (d). The weak relaxor nature of the BZT-xBCT ceramics suggests the presence of PNRs, which could considerably contribute to the ECE.

According to the Maxwell relation, the adiabatic temperature change ΔT can be deduced from the temperature dependence of polarization by: [23]

$$\Delta T = -\frac{T}{\rho\times Cp}\int_{E_1}^{E_2}\left(\frac{\partial P}{\partial T}\right)_E dE \qquad (1)$$

where T is the ambient temperature, ρ is the density, c_p is the specific heat capacity, P is the polarization and E_1 and E_2 are the starting and maximum applied electric fields, respectively.

The specific heat capacity c_p is assumed to be temperature independent in the temperature range of interest [0.46 (x = 0.3), 0.50 (x = 0.4), 0.48 (x = 0.5), 0.53 (x = 0.6) and 0.52 (x = 0.7) J mol^{-1} K^{-1}]. The values of $\left(\frac{\partial P}{\partial T}\right)_E$ were estimated from P_{max} - T data by a fourth order polynomial fit. In addition, the electrocaloric coefficient ($\xi = \frac{\Delta T}{\Delta E}$) is introduced as a normalized parameter to evaluate the ECE in different materials because this parameter is independent of geometrical shape and size of the sample.[5,24,25]

Fig.4 (a) - (e) show the plots of calculated ΔT as a function of temperature of BZT-xBCT ceramics for ΔE varying from 5 to 28 kV/cm (E_1 = 0). Three important insights can be gained from the temperature and electric field dependence of ΔT: (1) In addition to the usual positive electrocaloric effect, a slightly negative ECE at low temperature regions is also observed in BCT-rich compositions, i.e. x ≥ 0.5. A similar coexistence of a positive and negative ECE, though it is a rare case, was also observed in Pb(Mg$_{2/3}$Nb$_{1/3}$)O$_3$-xPbTiO$_3$ and Bi$_{1/2}$Na$_{1/2}$TiO$_3$-xBaTiO$_3$ relaxor ferroelectrics with compositions near MPB. [26,27] Theoretical study pointed out that the cause of this dual nature of the ECE in the same material at different temperatures may be the two phase transitions very close in temperature.[28] However, this may not be strictly the case for our BZT-xBCT ceramics. Though the origin of negative ECE is not completely clear, it should be closely related to the tetragonal - rhombohedral phase transition as indicated in Fig.3 (a); (2) The maximum of electrocaloric effect (denoted by T_{EC}) is found near the dielectric constant maximum temperature at low fields. The T$_{EC}$ shifts from the proximity of T_m to higher temperatures above a certain composition-dependent electric field strengths. This effect is particularly significant at BZT-rich compositions, i.e. x ≤ 0.4. Such phenomenon has been found in many similar perovskite ferroelectrics [16,18] and is attributed to the field induced shift in the phase transition temperature;

[29,30] (3) The emergence of the broad $\Delta \boldsymbol{T}$ peaks slightly above the dielectric constant maximum temperature for all the compositions is directly associated with the relaxation process and entropy contribution of PNRs, which can appear a few hundred degrees above the phase transition temperature.[31] Therefore, the temperature and electric field evolution of ECE above T_m in different BZT-xBCT compositions can also be related to an increasing field-induced contribution from aligning and growing PNRs. The size, concentration and dynamics of PNRs are critical to this process.[12]

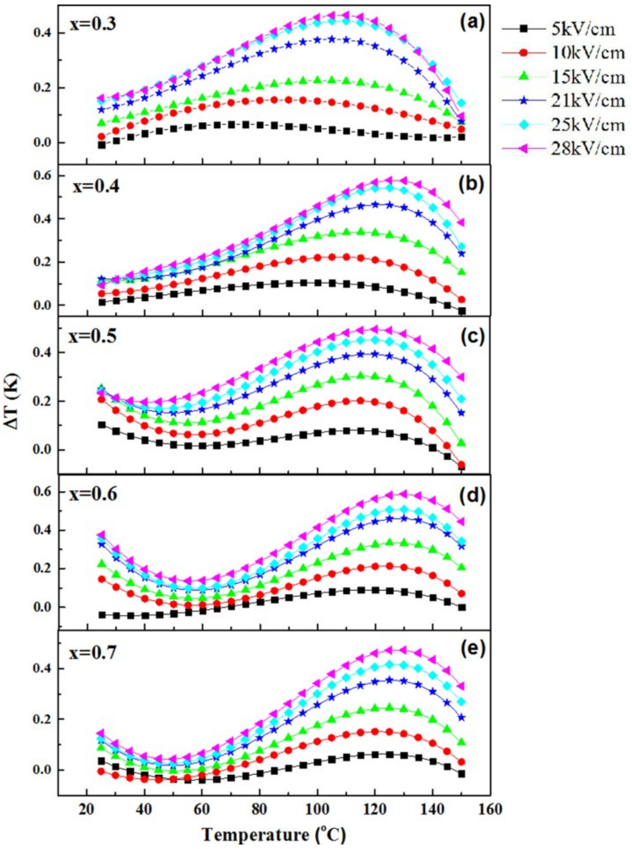

Fig.4 Electrocaloric temperature change (ΔT) in BZT-xBCT ceramics for (a) x = 0.3, (b) x = 0.4, (c) x = 0.5, (d) x = 0.6 and (e) x = 0.7 as a function of temperature and electric field.

The exactness of the indirect method has triggered an intensive scientific discussion over the past few years due to its limitations in determination of EC effect, in particular for relaxor systems since they show non-ergodic behaviour.[4,5] Eq. (1) in general is derived based on the assumption that the thermodynamic system is ergodic under adiabatic conditions. Despite the limitations of the indirect method, many groups still employed this approach to study the EC effect in various perovskite-type relaxors.[18,26,32-34] Therefore, we believe the indirect measurements can provide reasonably reliable information about the electrocaloric effect in our BZT-xBCT ceramics, given the nature of weak relaxor, relatively small hysteresis losses and coercive fields.[35,36]

Fig. 5 shows the compositional dependence of maximum electrocaloric temperature change (ΔT_{max}) and the electrocaloric coefficient ($\Delta T_{max}/\Delta E$) of BZT-xBCT ceramics. The maximum electrocaloric temperature change ΔT_{max} varies between 0.46 K (at 110 ℃ for BZT-0.3BCT) and 0.59 K (at 130 ℃ for BZT-0.6BCT) under an electric field of 28 kV/cm. Surprisingly, the room-temperature MPB composition (x = 0.5) doesn't exhibit the largest ECE as expected.[17,37] This could be a result of temperature-induced MPB shift or possible electric-field induced quasi second-order phase transition.[38] BZT-0.4BCT and BZT-0.6BCT show similar ECE with largest ΔT_{max} and $\Delta T_{max}/\Delta E$ over the investigated composition range. From a technical point of view, however, a smooth and uniform ECE over a broad temperature range is desired rather than the coexistence of both positive and negative ECE. To this end, BZT-0.4BCT is more promising for a simple solid state cooling device.

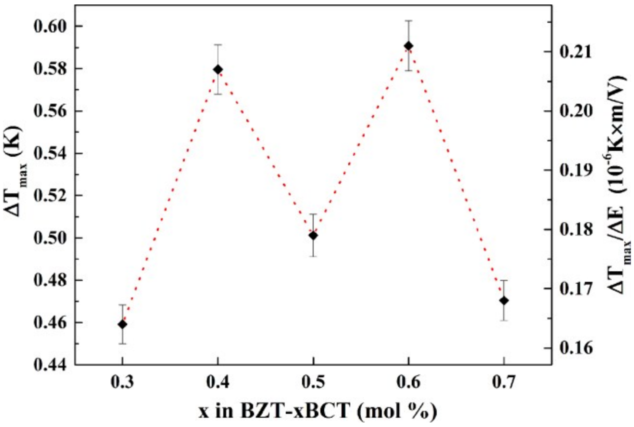

Fig.5 The maximum electrocaloric temperature change (ΔT_{max}) and the electrocaloric coefficient ($\Delta T_{max}/\Delta E$) under 28 kV/cm (ΔE = 28 kV/cm) as a function of composition x in the BZT-xBCT system. The line is drawn as a guide to the eyes.

Table I gives the comparison of the electrocaloric properties of the BZT-xBCT ceramics developed in this work and various lead-free materials, including ceramics, single crystals and polymers, reported in the literatures. As shown in Table I, our BZT-0.4BCT ceramic displays one of the highest electrocaloric responses in terms of the electrocaloric coefficient $\Delta T_{max}/\Delta E$ among the polycrystalline lead-free ferroelectric materials. However, the ECE strength of our ceramics is lower than that of the single crystals. This can be attributed to the single crystalline nature of the $BaTiO_3$ and $Sr_{0.61}Ba_{0.39}Nb_2O_6$ samples. It is also noted that the temperature (T_{EC}) of maximum ΔT in our BZT-0.4BCT ceramic is higher than those of many other lead-free counterparts, which is closer to room temperature. In general, the ECE should be strong over a wide temperature range close to the desired working temperature, enabling the realization of effective cooling cycles. Our BZT-0.4BCT would be more suitable to apply in devices functioning at elevated temperatures, e.g. ~ 100 ℃ for applications near car engines.

TABLE I. Comparison of our BZT-xBCT ceramics with other lead-free organic and inorganic EC counterparts.

Materials	T_{EC} (℃)	ΔT_{max} (K)	ΔE (kV/cm)	$\Delta T_{max}/\Delta E$ (10^{-6}K×m/V)	Measurement method
0.6BZT-0.4BCT ceramic(this work)	125	0.58	28	0.21	Indirect
$BaTi_{0.95}Sn_{0.05}O_3$ ceramic[39]	85	0.079	3.62	0.19	Indirect
0.65BZT-0.35BCT ceramic[15]	65	0.33	20	0.165	Direct DSC
0.7BZT-0.3BCT ceramic[17]	55	0.3	20	0.15	Indirect
$Ba_{0.98}Ca_{0.02}Zr_{0.085}Ti_{0.915}O_3$ ceramic[40]	85	0.6	40	0.15	Direct
0.92NBT-0.08BT ceramic[41]	100	0.2	40	0.05	Indirect
$K_{0.5}Na_{0.5}NbO_3$-$SrTiO_3$ ceramics[42]	67	1.9	159	0.12	Direct
0.45BZT-0.55BCT single crystal[16]	130.8	0.46	12	0.38	Indirect
$BaTiO_3$ single crystal[25]	129	0.9	12	0.75	Direct
Ce doped $Sr_{0.61}Ba_{0.39}Nb_2O_6$ single crystal[43]	100	1.1	28	0.39	Direct
P(VDF-TrFE) 55/45[3]	80	12.6	2090	0.06	Indirect
Irradiated P(VDF-TrFE) 68/32[20]	33	20	1600	0.125	Direct
P(VDF-TrFE-CFE) 59.2/33.6/7.2[44]	30	15	1500	0.1	Direct

Conclusions

In summary, electrocaloric effect in (1-x)$Ba(Zr_{0.2}Ti_{0.8})O_3$-x$(Ba_{0.7}Ca_{0.3})TiO_3$ ceramics was investigated as a function of composition, temperature and electric field by indirect polarization measurements. The temperature range and magnitude of the electrocaloric effect were greatly extended to temperatures higher than the dielectric constant maximum points above certain composition dependent electric field strengths due to the field induced shift in the phase transition temperature as well as contribution of polar nano-regions. Coexistence of an abnormal negative ECE and usual positive ECE became evident in BZT-xBCT with high x ($x \geq 0.5$). The low-temperature rhombohedral-tetragonal phase transition was presumably responsible to the observed dual nature of ECE. The most promising ECE was found in composition x = 0.4, which exhibited a monotonic positive ECE in the temperature range of interest, with a promising ΔT of 0.58 K at ~ 125 ℃ under a moderate electric field of 28 kV/cm, equivalent to a electrocaloric coefficient $\xi = 0.21 \times 10^{-6}$ K×m/V. The electrocaloric coefficient in our BZT-0.4BCT ceramic is among the highest ECE reported for lead-free materials in the literature up to this date, suggesting the intriguing possibility of high performance environmentally friendly solid-state cooling devices based on BZT-xBCT ceramics, particularly for military and automotive applications.

Acknowledgements

This work was supported by the Australian Research Council Discovery Project (Grant No. DP110104629). D. Y. Wang also acknowledges the financial support from State Key Laboratory of Electrical Insulation and Power Equipment, Xi'an Jiaotong University, China (Grant number EIPE15206). Q.R. Lin acknowledges the support from the CSC under Grant number 201206120021.

References

[1] S. Kar-Narayan and N. D. Mathur, Ferroelectrics 2012, **433**, 107.

[2] Y. Bai, G.P. Zheng, and S.Q. Shi, J. Appl. Phys. 2010, **108**, 104102.

[3] B. Neese, B. Chu, S.G. Lu, Y. Wang, E. Furman, and Q. M. Zhang, Science 2008, **321**, 821.

[4] J.F. Scott, Ann. Rev. Mater. Res. 2011, **41**, 229.

[5] M. Valant, Prog. Mater. Sci. 2012, **57**, 980.

[6] B. A. Tuttle and D. A. Payne, Ferroelectrics 1981, **37**, 603.

[7] Y. P. Shi and A. K. Soh, Acta Mater. 2011, **59**, 5574.

[8] R. Pirc, Z. Kutnjak, R. Blinc, and Q. M. Zhang, J. Appl. Phys. 2011, **110**, 074113.

[9] J. Hagberg, A. Uusimäki, and H. Jantunen, Appl. Phys. Lett. 2008, **92**, 132909.

[10] L.J. Dunne, M. Valan, A.K. Axelsson, G. Manos, and N.M. Alford, J. Phys. D. Appl. Phys. 2011, **44** , 375404.

[11] D. Guyomar,G. Sebald,B. Guiffard, and L. Seveyrat, J. Phys. D. Appl. Phys. 2006, **39**, 4491.

[12] J. Peräntie, H. N. Tailor, J. Hagberg, H. Jantunen, and Z.G. Ye, J. Appl. Phys. 2013, **114**, 174105.

[13] X. Hao, Z. Yue, J. Xu, S. An, and C.W. Nan, J. Appl. Phys. 2011, **110** , 064109.

[14] W.F. Liu and X.B. Ren, Phys. Rev. Lett. 2009, **103** , 257602.

[15] M. Sanlialp, V.V. Shvartsman, M. Acosta, B. Dkhil, and D.C. Lupascu, Appl. Phys. Lett. 2015, **106**, 062901.

[16] G. Singh, I. Bhaumik, S. Ganesamoorthy, R. Bhatt, A. K. Karnal, V. S. Tiwari, and P. K. Gupta, Appl. Phys. Lett. 2013, **102**, 082902.

[17] Y. Bai, X. Han, and L.J. Qiao, Appl. Phys. Lett. 2013, **102** , 252904.

[18] G. Singh, V. S. Tiwari, and P. K. Gupta, Appl. Phys. Lett. 2013, **103**,202903.

[19] A. S. Mischenko, Q. Zhang, J. F. Scott, R. W. Whatmore, and N. D. Mathur, Science 2006, **311**, 1270.

[20] S. G. Lu, B. Rožič, Q. M. Zhang, Z. Kutnjak, R. Pirc, M.R. Lin, X.Y. Li, and L. Gorny, Appl. Phys. Lett. 2010, **97**, 202901.

[21] J. Parui and S. B. Krupanidhi, Phys. Stat. Sol. (RRL) 2008, **2**, 230.

[22] A. A. Bokov and Z. G. Ye, J.Mater.Sci. 2006, **41**, 31.

[23] B. Neese, S. G. Lu, B. Chu, and Q. M. Zhang, Appl. Phys. Lett. 2009, **94** , 042910.

[24] G. Akcay, S. P. Alpay, J. V. Mantese, and G. A. Rossetti, Appl. Phys. Lett. 2007, **90**, 252909.

[25] X. Moya, E. Stern-Taulats, S. Crossley, D. González-Alonso,S. Kar-Narayan, A. Planes, L. Mañosa, and N.D. Mathur, Adv. Mater. 2013, **25**, 1360.

[26] S. Uddin, G.P. Zheng, Y. Iqbal, R. Ubic, and J. Yang, J. Appl. Phys. 2013, **114**, 213519.

[27] F. L. Goupil, A. Berenov, A.K. Axelsson, M. Valant, and N. M. Alford, J. Appl. Phys. 2012, **111**, 124109.

[28] A.K. Axelsson, F. L. Goupil, L. J. Dunne, G. Manos, M. Valant, and N. M. Alford, Appl. Phys. Lett. 2013, **102**, 102902.

[29] J. H. Qiu and Q. Jiang, J. Appl. Phys. 2009, **105**, 034110.

[30] B. Li, W. J. Ren, X. W. Wang, H. Meng, X. G. Liu, Z. J. Wang, and Z. D. Zhang, Appl. Phys. Lett. 2010, **96**, 102903.

[31] G.Y. Xu, J.S. Wen, C. Stock, and P. M. Gehring, Nature Mater. 2008, **7**, 562.

[32] R. Chukka, J. W. Cheah, Z.H. Chen, P. Yang, S. Shannigrahi, J. L. Wang, and L. Chen, Appl. Phys. Lett. 2011,**98** , 242902.

[33] G. Singh and V. S. Tiwari, J. Alloys. Compd. 2012, **523**, 30.

[34] B. Asbani, J.-L. Dellis, A. Lahmar, M. Courty, M. Amjoud, Y. Gagou, K. Djellab, D. Mezzane, Z. Kutnjak, and M. El Marssi, Appl. Phys. Lett. 2015, **106**, 042902.

[35] Y. Bai, X. Han, K. Ding, and L.J. Qiao, Appl. Phys. Lett. 2013, **103**, 162902.

[36] B. Rožič and Z. Kutnjak, Proceedings of the SEM Annual Conference. 2009.

[37] W. P. Cao, W. L. Li, D. Xu, Y. F. Hou, W. Wang, and W. D. Fei, Ceram. Int. 2014, **40**, 9273.

[38] H.Z Guo, B.K. Voas, S.J. Zhang, C. Zhou, X.B. Ren, S.P. Beckman, and X.L. Tan, Phys. Rev. B 2014, **90**, 014103.

[39] S.K. Upadhyay, V. R. Reddy, P. Bag, R. Rawat, S. M. Gupta, and A. Gupta, Appl. Phys. Lett. 2014, **105**, 112907.

[40] J.F. Wang, T.Q. Yang, S.C. Chen, G. Li, Q.F. Zhang, and X. Yao, J. Alloys Compd. 2013, **550**, 561.

[41] Y. Bai, G.P. Zheng, and S.Q. Shi, Mater. Res. Bull. 2011, **46**, 1866.

[42] J. Koruza, B. Rožič, G. Cordoyiannis, B. Malič, and Z. Kutnjak, Appl. Phys. Lett. 2015, **106**, 202905.

[43] F. L. Goupil, A.K. Axelsson, M. Valant, T. Lukasiewicz, J. Dec, A. Berenov, and N. M. Alford, Appl. Phys. Lett. 2014, **104**, 222911.

[44] X.Y. Li, X.S. Qian, S. G. Lu, J.P. Cheng, Z. Fang, and Q. M. Zhang, Appl. Phys. Lett. 2011, **99**, 052907.

RSC Advances

A table of contents entry: a graphic (maximum size 8 cm x 4 cm) and one sentence of text (maximum 20 words).

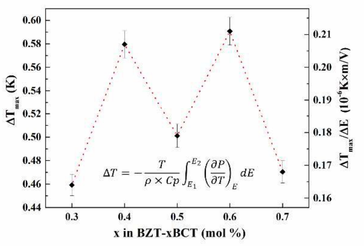

One sentence:

Compositional dependence of electrocaloric effect in lead-free BZT-xBCT ceramics (x = 0.3 - 0.7) were investigated using the indirect method.